

1 **Changes in hypothalamic subunits volume and their association with metabolic**
2 **parameters and gastrointestinal appetite-regulating hormones following bariatric**
3 **surgery**

4
5
6 **Amélie Lachance**^{1,2,3}, Justine Daoust^{1,2,3}, Mélissa Pelletier², Alexandre Caron², André C.
7 Carpentier⁴, Laurent Biertho⁵, Josefina Maranzano⁶, André Tchernof^{2,3}, Mahsa Dadar⁷,
8 Andréanne Michaud^{1,2,3}

9
10 **Affiliations**

11 1. Centre Nutrition, Santé et Société (NUTRISS), Institut sur la nutrition et les aliments fonctionnels (INAF),
12 Université Laval, Québec, Qc, G1V 0A6, Canada;

13 2. Institut universitaire de cardiologie et de pneumologie de Québec - Université Laval, Québec, Qc, G1V 4G5,
14 Canada;

15 3. École de nutrition, Faculté des sciences de l'agriculture et de l'alimentation, Université Laval, Québec, Qc,
16 G1V 0A6, Canada;

17 4. Centre de recherche du centre hospitalier universitaire de Sherbrooke, Université de Sherbrooke, Sherbrooke,
18 Qc, J1H 5N4, Canada;

19 5. Département de chirurgie générale, Institut universitaire de cardiologie et de pneumologie de Québec-
20 Université Laval, Québec, Qc, G1V 4G5, Canada;

21 6. Département d'anatomie, Université du Québec à Trois-Rivières, Trois-Rivières, Qc, G8Z 4M3, Canada;

22 7. Douglas Research Centre, Université McGill, Montréal, Qc, H4H 1R3, Canada.

23 **Corresponding author:** Andréanne Michaud, R.D., Ph.D. Address: 2725, Chemin Ste-Foy,
24 Québec (QC), Canada, G1V 4G5. E-mail: andreanne.michaud@criucpq.ulaval.ca

25

26

27 **Abstract**

28

29 **Background:** Some nuclei of the hypothalamus are known for their important roles in
30 maintaining energy homeostasis and regulating food intake. Moreover, obesity has been
31 associated with hypothalamic inflammation and morphological alterations, as indicated by
32 increased volume. However, the reversibility of these changes after bariatric surgery-induced
33 weight loss remains underexplored. **Objective:** The aim of this study was to characterize
34 volume changes in hypothalamic subunits up to two years following bariatric surgery and to
35 determine whether these differences were associated with changes in metabolic parameters
36 and levels of gastrointestinal appetite-regulating hormone levels. **Methods:** Participants with
37 severe obesity undergoing bariatric surgery were recruited. They completed high-resolution
38 T1-weighted brain magnetic resonance imaging (MRI) before bariatric surgery and at 4, 12
39 and 24 months post-surgery. Blood samples collected during the fasting and postprandial
40 states were analyzed for glucagon-like peptide 1 (GLP-1), peptide YY (PYY), and ghrelin
41 concentrations. The hypothalamus was segmented into 5 subunits per hemisphere using a
42 publicly available automated tool. Linear mixed-effects models were employed to examine
43 volume changes between visits and their associations with variables of interest. **Results:** A
44 total of 73 participants (mean age 44.5 ± 9.1 years, mean BMI 43.5 ± 4.1 kg/m²) were
45 included at baseline. Significant volume reductions were observed in the whole left
46 hypothalamus 24 months post-surgery. More specifically, decreases were noted in both the
47 left anterior-superior and left posterior subunits at 12 and 24 months post-surgery (all $p < 0.05$,
48 after FDR correction). These reductions were significantly associated with the percentage of
49 total weight loss (both subunits $p < 0.001$), improvements in systolic blood pressure (both
50 subunits $p < 0.05$), and an increase in postprandial PYY (both subunits $p < 0.05$). **Conclusion:**
51 These results suggest that some hypothalamic morphological alterations observed in the
52 context of obesity could potentially be reversed with bariatric surgery induced-weight loss.

53

54

55 **Keywords:** hypothalamus, structural MRI, volumetric study, segmentation, bariatric surgery,
56 gastrointestinal appetite-regulating hormones

57

58

59

60

61

62

63

64

65 **1 Introduction**

66

67 Food intake involves a complex, simultaneous interplay of various brain regions (Dagher,
68 2012). Despite its modest 1% contribution to total brain weight on average, the hypothalamus
69 plays a central role in regulating this process (Dagher, 2012; Clifford B. Saper, 2012). Acting
70 as a control center, it integrates signals from a myriad of afferent nerves within the body and
71 coordinates their transmission to cortical and subcortical grey matter (C. B. Saper & Lowell,
72 2014). Therefore, the hypothalamus contributes to several critical biological mechanisms
73 essential for basic survival functions, including energy metabolism and the homeostatic
74 control of food intake (C. B. Saper & Lowell, 2014). These functions are orchestrated by a
75 dozen specific nuclei within the hypothalamus, which are characterized by distinct cellular
76 populations (Bedont, Newman, & Blackshaw, 2015; Billot et al., 2020; Xie & Dorsky, 2017).
77 Among these are the arcuate, lateral, paraventricular, dorsomedial and ventromedial nuclei,
78 all implicated in the regulation of food intake (Caron & Richard, 2017).

79

80 Given its fundamental role in metabolic homeostasis, the hypothalamus has been extensively
81 studied to elucidate potential disruptions associated with obesity. Most of these studies have
82 been conducted in animal models, with relatively limited investigations conducted in humans.
83 Challenges associated with the small size of the hypothalamus have limited the use of
84 magnetic resonance imaging (MRI) techniques until recent advancements. Manual
85 delineation of its boundaries, which requires expertise and a valuable amount of time
86 (Schindler et al., 2013), has now been supplanted by the development of automated
87 segmentation techniques, facilitating the study of larger cohorts (Billot et al., 2020;
88 Rodrigues et al., 2022). The automated segmentation tool developed by Billot *et al.* divides

89 the hypothalamus into five subunits per hemisphere, offering nuanced insights into its
90 functioning (Billot et al., 2020). Using this tool, two recent studies showed morphological
91 alterations in the hypothalamus among individuals living with overweight or obesity, with
92 increased volume for the whole hypothalamus and for specific subunits (Alzaid et al., 2024;
93 Brown, Westwater, Seidlitz, Ziauddeen, & Fletcher, 2023). However, the mechanisms
94 underlying these findings and whether these hypothalamic alterations in individuals with
95 obesity are permanent or reversible following interventions targeting weight loss and
96 cardiometabolic improvements remain unexplored.

97

98 Bariatric surgery, known for inducing significant and sustained weight loss alongside
99 metabolic improvements, presents a unique opportunity to study long-term effects on brain
100 integrity in a prospective setting (Maciejewski et al., 2016; O'Brien et al., 2019; Salminen et
101 al., 2022). Significant changes in both white and grey matter densities have been documented
102 post-bariatric surgery (Michaud et al., 2020; Rullmann et al., 2018; Tuulari et al., 2016;
103 Wang et al., 2020). Previous studies have also examined the impact of bariatric surgery on
104 hypothalamic morphological changes using voxel-based morphometry (VBM), with only one
105 reporting volume changes in specific subregions (Rullmann et al., 2019; van de Sande-Lee et
106 al., 2020). A recent study employing an automated segmentation tool, which is considered
107 more reliable than VBM techniques for assessing volume in such a small region of the brain
108 (Arkink et al., 2017), demonstrated reductions in hypothalamic volume one year post-
109 surgery, particularly in different subunits of the left hypothalamus (Pané et al., 2024).
110 However, a study with longer-term follow-up is needed to explore the sustainability of the
111 effects of weight-loss and concomitant cardiometabolic improvements on hypothalamic
112 morphometric changes.

113

114 The mechanisms underlying hypothalamic morphological alterations in the context of obesity
115 remain unclear. Various hypotheses have been explored over the years, including
116 hypothalamic inflammation and gliosis (Schur et al., 2015; Sewaybricker, Huang,
117 Chandrasekaran, Melhorn, & Schur, 2023; Thaler, Guyenet, Dorfman, Wisse, & Schwartz,
118 2013) as well as a decreased level of brain vascularization and cerebral hypoperfusion
119 (Alfaro et al., 2018; Bettcher et al., 2013; Willeumier, Taylor, & Amen, 2011). Some
120 gastrointestinal hormones could also play a role in the remodeling process of the
121 hypothalamus, as they exert their effects by binding to receptors within the hypothalamus (Al
122 Massadi, López, Tschöp, Diéguez, & Nogueiras, 2017; Farr et al., 2016; Jensen et al., 2018;
123 Karra, Chandarana, & Batterham, 2009; Li et al., 2023) or by acting on neurons projecting
124 into hypothalamic nuclei (Biddinger, Lazarenko, Scott, & Simerly, 2020). Moreover,
125 concomitant changes in hunger and satiety hormones, such as ghrelin, glucagon-like peptide
126 1 (GLP-1), and peptide YY (PYY), have been reported in obesity (Aukan, Coutinho,
127 Pedersen, Simpson, & Martins, 2023) and following bariatric surgery (Huang et al., 2023). It
128 remains unknown how changes in peripheral gut hormones are associated with hypothalamic
129 morphometric changes following bariatric surgery.

130

131 In this prospective study, we aimed to characterize changes in hypothalamic volume and its
132 subunits up to two years following bariatric surgery by employing an automated
133 segmentation tool (Billot et al., 2020). As a secondary objective, we examined whether these
134 changes were associated with weight loss, metabolic parameters, and variations in
135 gastrointestinal appetite-regulating hormone levels, including ghrelin, GLP-1, and PYY. We
136 hypothesized that bariatric surgery leads to reductions in total hypothalamus volume and
137 specific subunits, and these changes are associated with the magnitude of weight loss, as well

138 as improvements in cardiometabolic parameters and gastrointestinal appetite-regulating
139 hormone levels.

140

141 **2 Methods**

142 **2.1 Participants**

143

144 Ninety-two participants scheduled to undergo bariatric surgery at the *Institut universitaire de*
145 *cardiologie et de pneumologie de Québec-Université Laval (IUCPQ-UL)* in Québec, Canada,
146 were recruited (Figure S1). These participants were part of a larger prospective study, which
147 aimed at investigating the determinants of metabolic recovery following bariatric surgeries.
148 The protocol has been previously described in detail (Michaud et al., 2020). Briefly,
149 participants had to be 18 to 60 years old and meet the NIH Guidelines for bariatric surgery
150 ("Gastrointestinal surgery for severe obesity: National Institutes of Health Consensus
151 Development Conference Statement," 1992). Exclusion criteria included gastrointestinal
152 diseases, such as irritable bowel syndrome or gastro-intestinal ulcers, cirrhosis or albumin
153 deficiency, neurological illnesses, uncontrolled high blood pressure, use of any medication
154 that can affect the central nervous system, previous bariatric or brain surgery, severe food
155 allergy, current pregnancy and substance or alcohol abuse. Participants with any
156 contraindications for MRI, including claustrophobia, metal embedded in the body, or the
157 presence of an implanted medical device, were also excluded. The protocol was approved by
158 the Research Ethics Committee of the *Centre de recherche de l'IUCPQ-UL* (no. 2016-2569,
159 21237). A written consent form was signed by each participant at their first visit.

160 **2.2 Surgical procedures**

161 Participants received either a sleeve gastrectomy (SG), a Roux-en-Y gastric bypass (RYGB)
162 or a biliopancreatic diversion with duodenal switch (BPD-DS). All surgeries were performed

163 laparoscopically. Regarding SG, a 250 cm³ vertical gastrectomy was performed with a 34-44
164 French Bougie starting 7-8 cm from the pylorus to the His angle (Biertho et al., 2016). For
165 the RYGB, a 30-50 cm³ proximal gastric pouch was first created and then connected to the
166 proximal small intestine by bypassing the first 100 cm (Zeighami et al., 2021). Finally, the
167 BPD-DS was performed by first doing a 250 cm³ SG and thereafter, the duodenum was
168 transected about 4 cm distal from the pylorus and anastomosed to a 250-cm alimentary limb,
169 with a 100-cm common channel (Biertho et al., 2010).

170 **2.3 Study design and experimental procedures**

171 Outcomes were assessed prior to the surgery, and at 4, 12, and 24 months post-op. An
172 identical protocol was followed at each visit. Participants were asked to fast for 12 hours
173 before the visit. Weight and body composition were measured by bioimpedance (InBody520,
174 body composition analyzer, Biospace, Los Angeles, California or Tanita DC-430U, Arlington
175 Heights, IL). Anthropometric measures (waist, hip, and neck circumferences) and blood
176 pressure [systolic (SBP) and diastolic (DBP)] were measured using standardized procedures
177 (Michaud et al., 2020). The percentage of total weight loss (%TWL; [(baseline weight -
178 follow-up weight)/baseline weight] x 100%) and the percentage of excess weight loss
179 (%EWL; [(baseline weight - follow-up weight)/(pre-surgery weight – ideal weight for a body
180 mass index (BMI) of 23 kg/m²)] x 100%) were calculated.

181 **2.4. Plasma lipid profile, glucose homeostasis, and gastrointestinal appetite- 182 regulating hormones**

183 Blood samples were taken after a 12-hour overnight fast and approximately one hour after the
184 consumption of a standard nutritional beverage [237 ml Boost Original, Nestlé Health
185 Science (240 kcal, 41g of carbohydrates, 10g of proteins and 4g of lipids)]. Blood samples
186 were collected into chilled tubes with appropriate enzymatic inhibitors (dipeptidyl peptidase-
187 IV inhibitor, aprotinin, or HCl) (Millipore Sigma Canada, Ontario). All samples were

188 immediately kept at 4°C before being centrifuged, and then stored at -80°C. Fasted acylated
189 and non-acylated ghrelin were measured using ELISA kits (Bertin Pharma; A05106 and
190 A05119, respectively) and summed to obtain total ghrelin. Levels of post-prandial GLP-1 and
191 postprandial PYY were measured by multiplex assay (Millipore Sigma Canada, Ontario;
192 HMH3-34K) (Richard et al. 2022). Plasma levels of cholesterol, high-density lipoproteins
193 (HDL), low-density lipoproteins (LDL), triglycerides, glucose and insulin were measured at
194 each visit as part of the routine monitoring of patients. The homeostatic model assessment for
195 insulin resistance (HOMA-IR) was calculated [fasting glucose (mmol/L) x fasting insulin
196 (pmol/L) / 135) (Matthews et al., 1985).

197 **2.5 MRI acquisition**

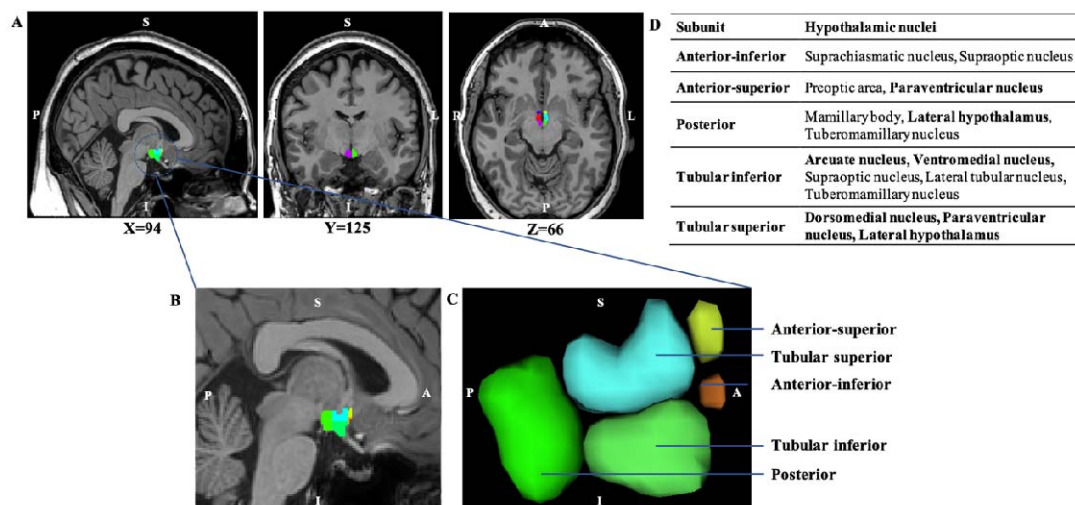
198 T1-weighted three-dimensional (3D) turbo echo images of the brain were acquired using a 3T
199 whole-body MRI scanner (Philips, Ingenia, Philips Medical Systems) equipped with a 32-
200 channel head coil at the *Centre de recherche de l'UCPQ-UL*. The following parameters were
201 used: 176 sagittal 1.0 mm slices, TR/TE = 8.1/3.7 ms, field of view (FOV) = 240 x 240 mm²,
202 and voxel size = 1 x 1 x 1 mm.

203 **2.6 MRI data analysis and hypothalamus segmentation**

204 Standard preprocessing steps, including image denoising (Coupe et al., 2008), intensity non
205 uniformity correction (Sled, Zijdenbos, & Evans, 1998) and image intensity normalization
206 into range (0–100) using histogram matching, were first applied. Images were then linearly
207 (using a nine-parameter rigid registration) registered to an average brain template (MNI
208 ICBM152-2009c) using MNI MINC tools
209 (<http://www.bic.mni.mcgill.ca/ServicesSoftware/MINC>). This step maps all the participants'
210 brain onto the same standard space, improving the performance of the downstream
211 segmentation pipeline and eliminating the need to adjust for total intracranial volume. All

212 registrations were visually controlled to ensure their accuracy. Segmentation of the
213 hypothalamus was performed on these standardized images using an open source method
214 based on a deep convolutional neural network (Billot et al., 2020). This automated
215 segmentation tool has been previously validated and used to perform hypothalamus
216 segmentation in similar applications (Alzaid et al., 2024; Brown et al., 2023; Pané et al.,
217 2024; Ruzok et al., 2022), and is part of the FreeSurfer brain segmentation software. This tool
218 allows the segmentation of the hypothalamus in 5 subunits per hemisphere: anterior-inferior,
219 anterior-superior, posterior, tubular inferior and tubular superior (Figure 1). Each of these
220 subunits includes two to five hypothalamic nuclei. Using FSLEyes, a tool from the FMRIB
221 Software Library (Jenkinson, Beckmann, Behrens, Woolrich, & Smith, 2012), every
222 individual segmentation (n=245) was visually inspected for quality control based on a
223 protocol published by Bochetta *et al.* (Bocchetta et al., 2015). Segmentations with irregular
224 shapes (n=56), such as holes and fragmented subunits, were considered low quality and were
225 excluded from further analyses (Figure S1). Additionally, we created a segmentation quality
226 variable that we included as a covariate in our statistical models to further assess the
227 robustness of our results. Images showing overall good segmentation but with minor defects,
228 such as some missing a few voxels lining the 3rd ventricle, were classified as moderate-
229 quality segmentations (n=64) but were still included in the analyses. The remaining
230 segmentations were classified as high-quality (n=125).

231



232

233

234 **Figure 1. Visual representation of the hypothalamic segmentation** A) Sagittal, Coronal and
 235 Axial brain slices showing hypothalamic segmentation and different hypothalamic subunits. B) Expanded view
 236 of the sagittal plane showing the left hypothalamus. C) Three-dimensional view of the left hypothalamus. D)
 237 Tables presenting the five hypothalamic subunits, and the corresponding hypothalamic nuclei included within
 238 them. Principal nuclei involved in food intake are highlighted in bold. 'L' denotes left, and 'R' denotes right. 'P'
 239 denotes posterior, and 'A' denotes anterior.

240 2.7 Statistical analyses

241 Participants' demographic data, cardiometabolic variables, and changes in gastrointestinal
 242 appetite-regulating hormones following bariatric surgery were assessed using Chi-squared
 243 tests for categorical variables and linear mixed-effects models for continuous variables.
 244 Linear mixed-effects models (Model I) were performed to examine hypothalamic volume
 245 changes following bariatric surgery. Participants were identified as categorical random
 246 variables, and age, sex, initial BMI, surgery type and session were added as fixed effects.

247 **Model I:** Hypothalamic volume ~ Session + Age + Sex + BMI_{baseline} + Surgery type + (1|
 248 Participant)

249

250 Linear mixed-effects models (Model II) were used to examine the associations between the
 251 changes in cardiometabolic variables (total weight loss, percentage of fat mass, SBP, HOMA-
 252 IR, plasmatic levels of triglycerides and HDL-C), and total left and right hypothalamus

253 volume and their subunits. Participants were added to the model as categorical random
254 variables, and age, sex, initial BMI and surgery type as fixed effects.

255 **Model II:** Hypothalamic volume ~ cardiometabolic variable + Age + Sex + BMI_{baseline} +
256 Surgery type + (1| Participant)

257

258 Linear mixed-effects models (Model III) were also used to examine the associations between
259 the changes in gastrointestinal appetite-regulating hormones (fasting total ghrelin and
260 acylated ghrelin, as well as postprandial GLP-1 and PYY) and total left or right
261 hypothalamus volume and their subunits. Participants were added to the model as categorical
262 random variables, and age, sex, initial BMI and surgery type as fixed effects.

263 **Model III:** Hypothalamic volume ~ gastrointestinal appetite-regulating hormones + Age +
264 Sex + BMI_{baseline} + Surgery type + (1| Participant)

265 The variables referred to as “cardiometabolic variable” or “gastrointestinal appetite-
266 regulating hormones” in Models II and III represent the prospective measurements of the
267 absolute levels of each variable, collected and entered for all time points. Due to the limited
268 sample size and multicollinearity, the effect of each cardiometabolic or hormonal variable
269 was examined separately.

270

271 Additional analyses were conducted to determine if segmentation quality significantly
272 impacted the results. First, volumes of high-quality segmentations were compared to volumes
273 of moderate-quality segmentations for each visit separately. T-tests were used for normally
274 distributed variables with equal variance, whereas Welch’s tests were used for unequal
275 variance. Variables not following a normal distribution were first transformed (log or
276 BoxCox transformation). If a normal distribution could not be achieved after transformations,
277 a non-parametric test (Wilcoxon test) was used. Furthermore, the segmentation quality

278 variable was integrated as a fixed effect covariate in Model I to determine if segmentation
279 quality (high versus moderate) significantly impacted the results.

280

281 All results were corrected for multiple comparisons with the False Discovery Rate (FDR)
282 controlling approach ($p < 0.05$) using the Benjamini-Hochberg procedure. Statistical analyses
283 were performed using JMP Pro version 16.0 (SAS Institute Inc., Cary, NC, USA).

284 **3 Results**

285 **3.1 Clinical characteristics of the participants**

286 Table 1 shows the characteristics of the participants. After quality control of the
287 hypothalamus segmentations, a total of 73 participants (mean age 44.5 ± 9.1 years, mean
288 BMI 43.5 ± 4.1 kg/m²) were included at baseline (Figure S1). The study population consisted
289 mainly of females (71%). SG was the most frequently performed procedure. As expected,
290 participants had significant weight loss following bariatric surgery ($p < 0.0001$). They also
291 showed improvements in blood pressure (systolic and diastolic, both $p < 0.0001$),
292 improvements in glucose homeostasis markers (fasting glycemia, fasting insulin, and
293 HOMA-IR index, all $p < 0.0001$) and lipid profile (total cholesterol, $p = 0.009$; HDL-C, $p <$
294 0.0001 ; and triglycerides, $p < 0.0001$). Total and acylated fasting ghrelin levels were
295 significantly decreased post-surgery (both $p < 0.0001$), while postprandial GLP-1 and PYY
296 levels were significantly increased ($p = 0.029$ and $p < 0.0001$, respectively).

297

298
299
300

Table 1. Characteristics of participants

	Baseline	4 months	12 months	24 months	p value
N	73	60	34	22	—
Age (years)	44.5 ± 9.1	—	—	—	—
Sex (F : M)	52 : 21	—	—	—	—
Type of surgery					
SG	47	42	20	13	—
RYGB	10	9	8	5	—
BPD-DS	16	9	6	4	—
Diabetes n (%)	19 (26)	17 (28)	10 (29)	5 (23)	0.942 ^a
Weight (kg)	121.1 ± 14.6	98.1 ± 12.0	80.8 ± 12.4	81.9 ± 16.5	<0.0001 ^b
BMI (kg/m ²)	43.5 ± 4.1	34.2 ± 3.7	29.6 ± 4.5	29.3 ± 4.7	<0.0001 ^b
Waist circumference (cm)	129.8 ± 10.2	111.4 ± 10.3	100.4 ± 11.1	99.2 ± 11.9	<0.0001 ^b
Percentage of body fat mass (%)	47.0 ± 6.3	42.6 ± 7.7	36.8 ± 8.7	37.3 ± 8.4	<0.0001 ^b
Total weight loss (%)	—	21.6 ± 4.0	32.8 ± 7.7	33.7 ± 7.9	<0.0001 ^b
Excess weight loss (%)	—	46.7 ± 9.9	70.0 ± 17.1	71.9 ± 16.9	<0.0001 ^b
SBP (mm Hg)	136 ± 16	123 ± 13	119 ± 12	119 ± 11	<0.0001 ^b
DBP (mm Hg)	81 ± 11	74 ± 10	74 ± 11	71 ± 9	<0.0001 ^b
Fasting glycemia [§] (mmol/L)	6.3 ± 1.7	5.2 ± 1.0	4.8 ± 0.8	4.9 ± 0.8	<0.0001 ^b
Fasting insulin [§] (mU/L)	175.1 ± 95.7	69.0 ± 40.5	50.9 ± 34.5	41.4 ± 21.3	<0.0001 ^b
HOMA-IR index [§]	8.4 ± 5.5	2.8 ± 2.1	1.9 ± 1.6	1.6 ± 0.9	<0.0001 ^b
Total cholesterol (mmol/L)	4.6 ± 0.9	4.0 ± 1.1	4.2 ± 0.8	4.4 ± 0.8	0.009 ^b
LDL-cholesterol (mmol/L)	2.6 ± 0.8	2.3 ± 1.0	2.3 ± 0.8	2.2 ± 0.7	0.217 ^b
HDL-cholesterol (mmol/L)	1.2 ± 0.3	1.2 ± 0.3	1.4 ± 0.3	1.6 ± 0.4	<0.0001 ^b
Triglycerides (mmol/L)	1.7 ± 0.8	1.4 ± 1.2	1.1 ± 0.4	1.1 ± 0.4	<0.0001 ^b
Fasting ghrelin (pg/ml)					
Total [§]	309 ± 215	209 ± 116	200 ± 127	210 ± 153	<0.0001 ^b
Acylated [§]	61 ± 164	55 ± 166	31 ± 22	28 ± 14	<0.0001 ^b
Postprandial GLP-1 [§] (pmol/L)	84 ± 63	114 ± 73	96 ± 60	105 ± 76	0.029 ^b
Postprandial PYY (pmol/L)	31 ± 3	61 ± 5	66 ± 7	62 ± 9	<0.0001 ^b

Values are presented as mean ± standard deviation or n (%). F: female, M: male, SG: sleeve gastrectomy, RYGB: Roux-en-Y gastric bypass, BPD-DS: biliopancreatic derivation with duodenal switch, BMI: body mass index, SBP: systolic blood pressure, DBP: diastolic blood pressure, GLP-1: glucagon-like peptide 1, PYY: peptide YY. ^aChi-squared test, ^bMixed-effects models comparing baseline, 4 months, 12 months and 24 months post-surgery sessions, [§]Log transformed.

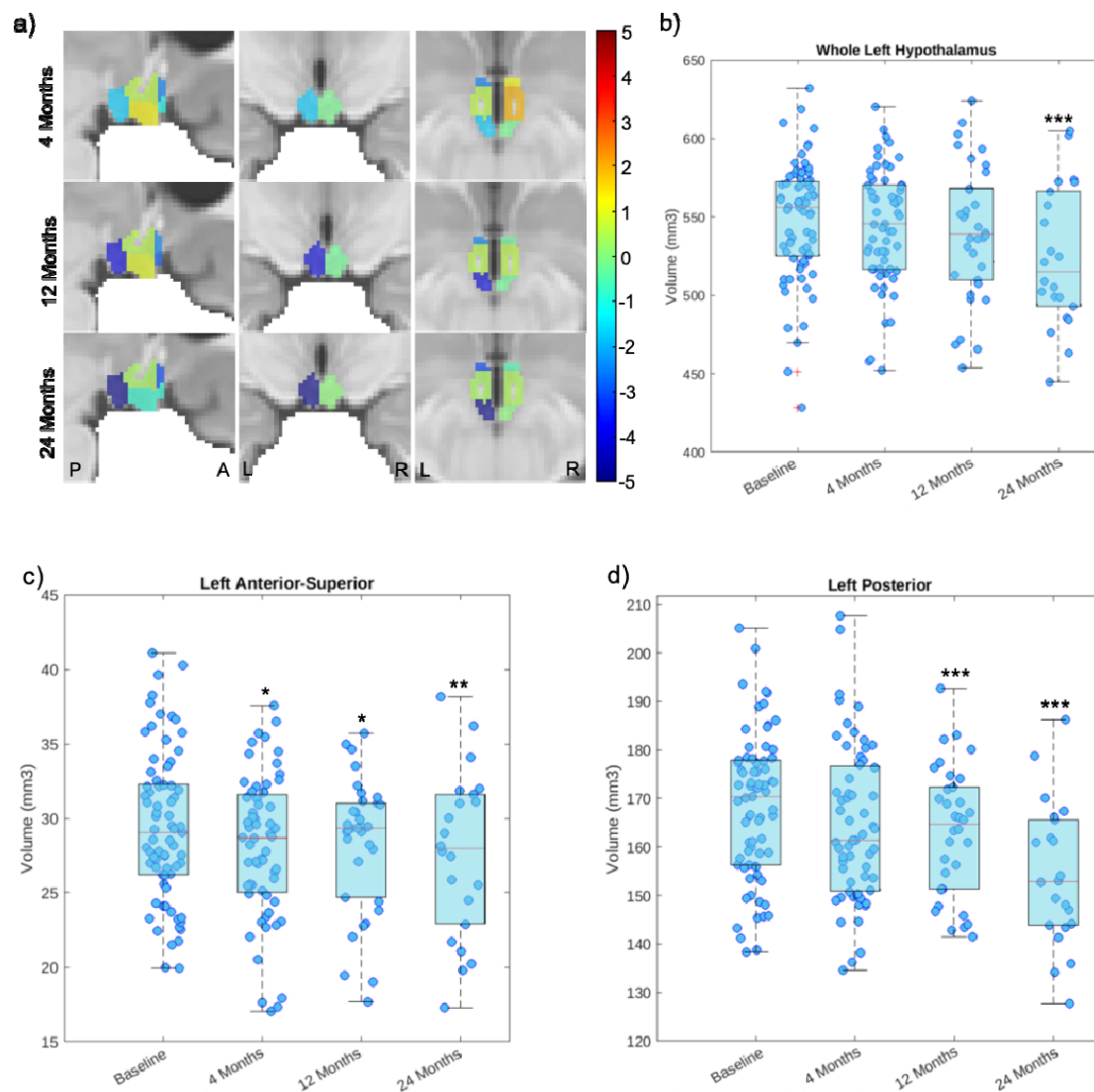
301
302
303

No significant differences in age, sex, and surgery type were observed between the high-quality segmentation group and the moderate-quality segmentation group for all sessions

304 (Table S1). However, participants in the moderate-quality segmentation group had a higher
305 BMI at baseline and a lower total weight loss at 12 months post-surgery compared to
306 participants in the high-quality segmentation group ($p=0.0307$ and $p=0.0226$, respectively;
307 Table S1). A higher percentage of participants with Type 2 diabetes was observed in the
308 high-quality segmentation group compared to the moderate-quality group at 4 months post-
309 surgery ($p=0.0027$, Table S1).

310 **3.2 Hypothalamic volume changes following bariatric surgery**

311 Figure 2a shows the T-values from the mixed effects-models (Model I), contrasting the
312 follow-up regional volumes against their baseline values. A significant decrease in the whole
313 volume of the left hypothalamus was observed 24 months post-surgery compared to baseline
314 ($p = 0.0007$, Figure 2b). More specifically, a local decrease in volume was observed in the
315 left anterior-superior subunit 4 months post-surgery compared to baseline ($p < 0.05$ after FDR
316 correction; Figure 2c). This decrease in volume was maintained at 12 months and 24 months
317 post-surgery ($p < 0.05$ and $p < 0.01$ after FDR correction; Figure 2c). Additionally, a
318 significant decrease in the volume of the left posterior subunit was also observed 12 and 24
319 months post-surgery compared to baseline (both $p < 0.001$ after FDR correction, respectively;
320 Figure 2d). No significant changes in volume were found in the right hypothalamus and its
321 subunits following bariatric surgery. When comparing the volumes of the left and right
322 hypothalamus and their subunits of the high- and moderate-quality groups at each visit, the
323 only significant difference between the two groups was for the whole left hypothalamus
324 (Table S2). Participants in the moderate-quality segmentation group had, on average, a higher
325 volume than those in the high-quality segmentation group. No significant difference for the
326 other subunits was observed after FDR correction. Furthermore, adding the segmentation
327 quality variable as a fixed effect in Model I did not change the results regarding volume
328 changes for the left and right hypothalamus and their subunits (Table S3).



329

330 **Figure 2. Changes in hypothalamus subunits 4, 12 and 24 months following bariatric**
331 **surgery compared to baseline** Panel a) shows the T-values from the mixed-effects models, contrasting
332 the follow-up regional volumes against their baseline values. Warmer colors (e.g. orange and red)
333 indicate an increase after surgery, while colder colors (e.g. blue and purple) indicate a decrease after surgery. 'L'
334 denotes left, and 'R' denotes right. 'P' denotes posterior, and 'A' denotes anterior. Significant changes in volumes
335 are observed in b) the whole left hypothalamus, c) the left anterior-superior subunit and d) the left posterior subunit.
336 * $p < 0.05$, ** $p < 0.01$, *** $p < 0.001$ versus baseline.
337

338 3.3 Associations between changes in hypothalamic volumes and 339 cardiometabolic variables following bariatric surgery

340 We used a mixed-effects model (Model II) to examine the association between changes in
341 hypothalamic volumes and cardiometabolic variables. Significant associations were found
342 between the volume of the whole left hypothalamus and the percentage of total weight loss

343 ($\beta = -39.88$, $p = 0.0008$), as well as the percentage of fat mass ($\beta = 1.06$, $p = 0.0021$),
344 wherein a more pronounced decrease in hypothalamic volume was associated with greater
345 total weight loss and a reduced percentage of fat mass following bariatric surgery (Table 2).
346 Associations between the percentage of total weight loss and specific subunits were also
347 observed, including the left anterior-inferior ($\beta = -3.83$, $p = 0.0223$, after FDR correction),
348 left anterior-superior ($\beta = -5.47$, $p = 0.0002$, after FDR correction), and left posterior
349 subunits ($\beta = -20.08$, $p < 0.0001$, after FDR correction). Conversely, no significant
350 association was observed between changes in the volume of the right hypothalamus and
351 weight loss.

352

353 Reduced volumes in the whole left hypothalamus and in the left anterior-superior subunit
354 were associated with increased levels of HDL-C ($\beta = -18.37$, $p = 0.0153$ and $\beta = -2.61$, $p =$
355 0.0077 , respectively, after FDR correction; Table 2), suggesting that improvement in HDL-C
356 is associated with reduced volumes. No significant associations were found between
357 hypothalamic volumes and other lipid profile markers, including triglycerides, LDL-C and
358 total cholesterol (Table 2, results for LDL-C and total cholesterol not shown). Decreased
359 volumes in the left anterior-superior and left posterior subunits were associated with
360 reductions in systolic blood pressure ($\beta = 0.04$, $p = 0.0147$ and $\beta = 0.16$, $p = 0.0022$,
361 respectively, after FDR correction; Table 2). No significant associations were found between
362 change in hypothalamic volumes and indicators of glucose homeostasis, namely HOMA-IR,
363 fasting glycemia and fasting insulin (Table 2, results for glycemia and insulin not shown).

364

365

366
367
368
369

Table 2. Associations between changes in hypothalamic volumes and metabolic parameters following bariatric surgery

	Left								
	Whole left			Anterior-inferior			Anterior-superior		
	β	S.D.	<i>p-value</i>	β	S.D.	<i>p-value</i>	β	S.D.	<i>p-value</i>
% Total weight loss	-39.88	11.22	0.0008	-3.83	1.63	0.0223	-5.47	1.38	0.0002
% Fat mass	1.06	0.33	0.0021	0.10	0.05	0.0405	0.11	0.04	0.0082
HDL-C	-18.37	7.36	0.0153	-1.98	0.99	0.0488	-2.61	0.95	0.0077
Triglycerides	1.01	3.14	0.7484	0.41	0.47	0.3881	0.69	0.44	0.1204
Systolic blood pressure	0.24	0.13	0.0543	0.01	0.02	0.482	0.04	0.02	0.0147
HOMA-IR	0.29	0.45	0.5118	0.05	0.05	0.3782	0.08	0.06	0.1439
	Posterior			Tubular inferior			Tubular superior		
	β	S.D.	<i>p-value</i>	β	S.D.	<i>p-value</i>	β	S.D.	<i>p-value</i>
	% Total weight loss	-20.08	4.18	< 0.0001	-1.07	4.75	0.8234	-0.73	4.51
% Fat mass	0.51	0.12	0.0001	0.06	0.14	0.654	0.02	0.14	0.8893
HDL-C	-5.06	3.29	0.1270	5.27	3.08	0.1027	-4.47	2.69	0.1037
Triglycerides	1.62	1.33	0.2257	-0.35	1.57	0.828	-0.62	1.27	0.6284
Systolic blood pressure	0.16	0.05	0.0022	-0.05	0.05	0.3335	0.07	0.05	0.1872
HOMA-IR	0.19	0.13	0.1712	-0.14	0.20	0.4988	-0.02	0.17	0.9145
	Right								
	Whole right			Anterior-inferior			Anterior-superior		
	β	S.D.	<i>p-value</i>	β	S.D.	<i>p-value</i>	β	S.D.	<i>p-value</i>
% Total weight loss	-1.98	11.33	0.8621	-2.75	1.75	0.1207	0.12	1.84	0.9487
% Fat mass	0.16	0.30	0.6046	0.01	0.05	0.8037	0.01	0.05	0.8358
HDL-C	-5.75	8.05	0.4772	-1.33	1.18	0.2640	-1.04	1.22	0.3926
Triglycerides	-1.12	3.00	0.7094	0.66	0.48	0.1768	0.03	0.48	0.9559
Systolic blood pressure	-0.002	0.13	0.9882	0.03	0.02	0.1341	-0.005	0.02	0.804
HOMA-IR	-0.52	0.44	0.2405	-0.06	0.06	0.3415	-0.02	0.06	0.785
	Posterior			Tubular inferior			Tubular superior		
	β	S.D.	<i>p-value</i>	β	S.D.	<i>p-value</i>	β	S.D.	<i>p-value</i>
	% Total weight loss	-0.15	4.22	0.9719	-2.33	5.14	0.6522	5.86	5.62
% Fat mass	0.06	0.12	0.6268	0.12	0.15	0.4207	-0.02	0.16	0.8796
HDL-C	-0.89	3.26	0.7870	-0.20	3.69	0.9579	-5.65	3.70	0.1295
Triglycerides	-0.50	1.38	0.7177	-0.36	1.43	0.8028	-0.64	1.45	0.6582
Systolic blood pressure	-0.01	0.05	0.7708	-0.05	0.05	0.4009	-0.007	0.06	0.9015
HOMA-IR	-0.08	0.17	0.621	-0.19	0.17	0.2702	-0.04	0.20	0.8542

β values from the mixed-effects models for the whole hypothalamus and its subunits. Results that were significant after FDR correction ($p < 0.05$) are shown in bold. S.D. : Standard deviation, HOMA-IR: Homeostasis model assessment for insulin resistance, HDL-C : High density lipoprotein cholesterol.

370

371 3.4 Associations between hypothalamic volumes and gastrointestinal 372 appetitive hormone levels following bariatric surgery

373 A decreased volume in the left anterior-superior and in the left posterior subunits following
374 bariatric surgery was associated with an increase in postprandial PYY ($\square = -0.03$, $p = 0.0034$
375 and $\square = -0.10$, $p = 0.0001$, respectively, after FDR correction; Table 3). Only the volume

376 change in the right anterior-inferior subunit showed a positive association with changes in
 377 total ghrelin levels ($\beta = 1.71$, $p = 0.0055$, after FDR correction; Table 3), whereas no
 378 association was found with the acylated form of ghrelin. Reduced volumes in the whole right
 379 hypothalamus and in the right anterior-inferior subunit were negatively associated with
 380 changes in levels of postprandial GLP-1 ($\beta = -0.09$, $p = 0.0057$ and $\beta = -0.01$, $p = 0.0076$,
 381 respectively, after FDR correction; Table 3).

382
 383
 384
 385

Table 3. Associations between hypothalamic volumes and variations in gastrointestinal appetite-regulating hormone levels following bariatric surgery

Left									
	Whole left			Anterior-inferior			Anterior-superior		
	β	S.D.	<i>p-value</i>	β	S.D.	<i>p-value</i>	β	S.D.	<i>p-value</i>
Ghrelin, total	5.28	4.41	0.2337	0.39	0.56	0.4907	0.33	0.55	0.5516
Ghrelin, acylated	3.97	4.75	0.4043	0.12	0.56	0.8303	0.46	0.61	0.453
GLP-1	-0.04	0.03	0.2490	0.005	0.005	0.3266	-0.002	0.005	0.6376
PYY	-0.11	0.07	0.0918	0.007	0.009	0.4346	-0.03	0.009	0.0034
Right									
	Whole right			Anterior-inferior			Anterior-superior		
	β	S.D.	<i>p-value</i>	β	S.D.	<i>p-value</i>	β	S.D.	<i>p-value</i>
Ghrelin, total	1.44	4.5	0.75	1.71	0.61	0.0055	-0.02	0.60	0.9796
Ghrelin, acylated	1.20	4.84	0.8051	1.39	0.60	0.0234	0.31	0.61	0.6056
GLP-1	-0.09	0.03	0.0057	-0.01	0.005	0.0076	-0.001	0.005	0.7115
PYY	-0.07	0.07	0.2819	-0.01	0.01	0.1505	-0.001	0.01	0.8899
Left (continued)									
	Posterior			Tubular inferior			Tubular superior		
	β	S.D.	<i>p-value</i>	β	S.D.	<i>p-value</i>	β	S.D.	<i>p-value</i>
Ghrelin, total	1.50	1.79	0.4027	1.45	1.92	0.4545	-1.04	1.77	0.5567
Ghrelin, acylated	-0.57	1.92	0.7654	3.91	2.00	0.0538	-0.34	1.76	0.8488
GLP-1	-0.04	0.01	0.0119	-0.005	0.01	0.7087	-0.01	0.01	0.3292
PYY	-0.10	0.02	0.0001	0.01	0.03	0.6260	-0.03	0.03	0.2780
Right (continued)									
	Posterior			Tubular inferior			Tubular superior		
	β	S.D.	<i>p-value</i>	β	S.D.	<i>p-value</i>	β	S.D.	<i>p-value</i>
Ghrelin, total	-0.96	1.66	0.5665	2.22	1.88	0.2406	-1.11	1.80	0.5397
Ghrelin, acylated	-1.99	1.93	0.3038	2.15	1.99	0.2827	-0.62	1.82	0.7363
GLP-1	-0.02	0.01	0.0856	-0.03	0.01	0.0223	-0.02	0.01	0.1376
PYY	-0.03	0.03	0.3081	-0.02	0.03	0.4311	-0.02	0.03	0.4003

β values from the mixed-effects models for the whole hypothalamus and its subunits. Results that were significant after FDR correction ($p < 0.05$) are shown in bold. Ghrelin (total and acylated) was measured after a 12h fast, while GLP-1 and PYY were measured in postprandial. S.D. : Standard deviation. GLP-1 : glucagon-like peptide 1, PYY : peptide YY.

386
 387

388

389 **4 Discussion**

390 In this study, a tool based on a deep convolutional neural network was used to examine
391 hypothalamic volume changes following significant weight loss induced by bariatric surgery.
392 Our findings revealed reduced volumes of the whole left hypothalamus, specifically in the
393 left anterior-superior and left posterior subunits. These hypothalamic morphological changes
394 post-surgery were associated with the percentage of total weight loss, as well as with
395 improvements in cardiometabolic variables, namely HDL-C and SBP. We also examined the
396 associations between hypothalamic volume changes and gastrointestinal appetite-regulating
397 hormone levels to explore potential mechanisms underlying hypothalamic alterations. We
398 found that reduced volumes in the left anterior-superior and left posterior subunits were
399 associated with changes in PYY levels.

400

401 To our knowledge, only one recent study has assessed hypothalamic volume following
402 bariatric surgery using a deep convolutional neural network method (Pané et al., 2024). They
403 found reduced volume in the whole left hypothalamus and left subunits one-year post-
404 surgery, but no volume changes in the whole right hypothalamus, which aligns with our
405 findings. However, they reported more widespread changes in hypothalamic volumes
406 compared to our study. Their larger sample size one year post-surgery (56 participants), along
407 with differences in the types of bariatric surgeries performed and the proportion of female
408 and male participants, could potentially explain the variations in results. It is also possible
409 that our analyses were underpowered to capture differences in volumes of certain subunits
410 due to the smaller sample size, particularly at 24 months post-surgery.

411

412 The posterior subunit notably encompasses the lateral nuclei. The orexin neurons within these
413 nuclei are well known for their role in food intake (Toshinai et al., 2003). Studies have
414 reported bilateral increases in the posterior subunits in obesity (Alzaid et al., 2024; Brown et
415 al., 2023). However, our results show that only the volume of the left posterior subunit is
416 reduced following bariatric surgery, which is consistent with findings from a similar study
417 (Pané et al., 2024). This suggests that alterations observed in obesity are reversible only for
418 the left side. Lateralization of the hypothalamus has also been noted in other volumetric
419 studies (Pané et al., 2024; Ruzok et al., 2022) and in studies assessing hypothalamic
420 inflammation using other MRI techniques (Kreutzer et al., 2017; Schur et al., 2015; Thomas
421 et al., 2019). Moreover, pathways involving the hypothalamus and other cerebral components
422 participating in homeostatic feeding are suggested to be lateralized to the left side (Castro,
423 Cole, & Berridge, 2015; Kiss et al., 2020). Thus, this lateralization could potentially explain
424 why only the volume of the left posterior subunit decreases following bariatric surgery, as it
425 profoundly affects the balance of food intake.

426

427 Additionally, we found a reduced volume in the left anterior-superior subunit at 4, 12 and 24
428 months following bariatric surgery. Similar results were reported by Pané *et al.*, as they also
429 observed reduced volume in this subunit 12 months post-surgery (Pané et al., 2024). The left
430 anterior-superior subunit includes parts of the paraventricular nucleus, which plays a role in
431 food intake through second order neurons that receive projections from orexinergic neurons
432 expressing Neuropeptide Y(NPY)/ agouti-related peptide (AgRP) of the arcuate nucleus (Li
433 et al., 2023; Roger et al., 2021). Interestingly, evidence shows a higher total volume in the
434 anterior-superior subunits (including both left and right parts) in participants living with
435 obesity as compared to lean controls (Alzaid et al., 2024). However, another study found no
436 difference when examining the left and right sides independently (Brown et al., 2023). These

437 discordant results may be explained by the small size of this subunit. Segmentation of the
438 anterior-superior and anterior-inferior subunits is reported to have lower accuracy due to the
439 challenging boundary between them (Billot et al., 2020).

440

441 Few studies have reported increased hypothalamic volume of the tubular inferior subunit
442 among participants with obesity compared to those with normal BMI (Alzaid et al., 2024;
443 Pané et al., 2024). This subunit includes, amongst other, the arcuate nucleus and the
444 ventromedial nucleus, both known for their roles in homeostatic feeding. Our results showed
445 no significant volume differences in this subunit following bariatric surgery, contrasting with
446 another study that found decreased volume in individuals living with obesity but without type
447 2 diabetes, with no changes observed in those with type 2 diabetes (Pané et al., 2024). These
448 differences suggest that some clinical characteristics and inter-individual variability may
449 influence the reversibility of hypothalamic alteration in the arcuate nucleus in the short term,
450 which could explain the lack of volume changes observed in our study. The tubular inferior
451 subunit also includes four other nuclei, potentially explaining the absence of volume changes
452 post-surgery in our study. The absence of recuperation of this structure could also provide
453 insights into the mechanisms explaining frequent weight regain observed in the years
454 following bariatric surgery. Therefore, it is important to address this gap in our current
455 knowledge, and further studies should aim to determine whether these alterations can be
456 reversed over a longer period.

457

458 Several mechanisms have been proposed to explain hypothalamic alterations associated with
459 obesity. Most evidence points toward hypothalamic inflammation and gliosis, which have
460 been demonstrated in preclinical studies and confirmed in humans using neuroimaging
461 studies (Sewaybricker et al., 2023). Neuroinflammation is known to lead to production of
462 proteases and free radicals that can affect the integrity of multiple brain structures. For

463 instance, proteases could disrupt the tight junctions of the blood-brain barrier, leading to
464 buildup of extracellular fluid and subsequent increases in volume (Rosenberg & Yang, 2007).
465 This is consistent with the increased mean diffusivity in the hypothalamus observed in
466 obesity, which as been reported with concomitant increased volumes (Pané et al., 2024).
467 Moreover, alterations in perineuronal nets, an extracellular matrix protecting synapses, have
468 been observed in rodents on a high-fat, high-sugar diet (Reichelt, Hare, Bussey, & Saksida,
469 2019). Without the protection of perineuronal nets, neurons are more exposed to free radicals,
470 potentially leading to hypothalamic inflammation and increased volume. As bariatric surgery
471 leads to decreased systemic inflammation (Askarpour, Khani, Sheikhi, Ghaedi, & Alizadeh,
472 2019) and reduced hypothalamic inflammation (Hankir et al., 2019; Pané et al., 2024), this
473 reduction could explain the following decrease in hypothalamic volume post-surgery.
474 However, our study was not designed to explore the pathways underlying these volume
475 changes. Future studies are therefore needed to elucidate these intriguing mechanisms.

476
477 To our knowledge, our study is the first to explore the associations between hypothalamic
478 volume changes and gastrointestinal appetite-regulating hormone levels after bariatric
479 surgery.

480 We found that higher levels of PYY were associated with more pronounced reductions in the
481 left anterior-superior and left posterior subunits post-surgery. While the physiological
482 significance of these associations in our study is limited, it is interesting that previous studies
483 have demonstrated the presence of PYY in the paraventricular nucleus in humans using
484 immunocytochemistry (Morimoto et al., 2008). We also found a positive association
485 between total ghrelin levels and volume change in the right anterior-inferior subunit, as well
486 as a negative association between GLP-1 levels and volume change in the whole right
487 hypothalamus and in the right anterior-inferior subunit following bariatric surgery. This
488 direction of association is expected, as many hypothalamic subunit volumes, as well ghrelin

489 levels are known to decrease after bariatric surgery, whereas GLP-1 levels are known to
490 increase (Huang et al., 2023). A recent study also reported a correlation between total ghrelin
491 levels and the volume of the anterior-inferior subunit in individuals with obesity (Alzaid et
492 al., 2024). However, since no significant changes were observed in the subunits of the right
493 hypothalamus following bariatric surgery, these results need to be interpreted with caution.

494

495 Several limitations need to be acknowledged. The tool we used did not allow for the
496 segmentation of individual nuclei. Subunits include two to five nuclei, and some nuclei are
497 divided into two different subunits, thus restricting the interpretation of the results. Our study
498 did not include any peripheral or cerebral markers of inflammation, nor did it incorporate
499 MRI sequences to assess brain inflammation, a potentially critical mechanism suggested to
500 participate in the remodeling of the hypothalamus. Thus, we cannot assess the role of
501 inflammation in hypothalamic volume changes. While this is the first study to examine long-
502 term changes in hypothalamic structure and subregions following bariatric surgery using MRI
503 scans up to two years post-surgery, the cohort completing the full two-year follow-up was
504 relatively small. Nonetheless, our study is the first to assess segmentation quality and to
505 incorporate it into our analyses.

506 **5. Conclusion**

507 In conclusion, our study shows reductions in volumes of the left hypothalamus and some
508 specific left subunits following bariatric surgery, suggesting a recovery of hypothalamic
509 alterations associated with obesity. Volume reductions were observed in the left anterior-
510 superior subunit, which includes the paraventricular nuclei, and in the left posterior subunit,
511 housing the lateral nuclei. Both of these hypothalamic nuclei play crucial roles in regulating
512 homeostatic food intake. Our findings suggest that changes in the hypothalamus in post-

513 bariatric surgery may be involved in shifts that could influence food intake regulation and
514 potentially impact weight loss outcomes.

515

516 **Data and Code Availability:** The automated hypothalamus segmentation method is publicly
517 available at : https://github.com/BBillot/hypothalamus_seg. Data will be made available on
518 request.

519

520 **Author contributions:** Conceptualization: LB, AT, AM. Methodology: AL, JD, JF, MD,
521 AM, MD. Data collection (participants): MP, LB. Data analysis: AL, ACC, MD, AC, JM.
522 Writing – original draft preparation: AL, MD, AM. Writing – review and editing: AL, JD,
523 MP, AC, ACC, LB, JM, AT. MD, AM. Supervision: AT, AM.

524

525 **Funding:** This study is supported by a Team grant from the Canadian Institutes of Health
526 Research (CIHR) on bariatric care (TB2-138776) and an Investigator-initiated study grant
527 from Johnson & Johnson Medical Companies (Grant ETH-14-610). Funding sources for the
528 trial had no role in the design, conduct, or management of the study, in data collection,
529 analysis, or interpretation of data, or in the preparation of the present manuscript and decision
530 to publish. A. L. is the recipient of a scholarship from the Canadian Institutes of Health
531 Research and of a Master's Training Scholarships from *Fonds de la recherche du Québec*.
532 A.M. and M.D. are the recipient of a Research Scholars - Junior 1 award from the *Fonds de*
533 *la recherche du Québec – Santé*. A.C.C. holds the Canada Research Chair in Molecular
534 Imaging of Diabetes. The co-investigators and collaborators of the REMISSION study are
535 (alphabetical order): Bégin C, Biertho L, Bouvier M, Biron S, Cani P, Carpentier A, Dagher
536 A, Dubé F, Fergusson A, Fulton S, Hould FS, Julien F, Kieffer T, Laferrère B, Lafortune A,
537 Lebel S, Lescelleur O, Levy E, Marette A, Marceau S, Michaud A, Picard F, Poirier P,
538 Richard D, Schertzer J, Tchernof A, Vohl MC.

539

540 **Conflicts of interest statement:** A. T. and L.B. are recipients of research grant support from
541 Johnson & Johnson Medical Companies and Medtronic for studies on bariatric surgery and
542 the Research Chair in Bariatric and Metabolic Surgery at IUCPQ and Laval University,
543 respectively. No author declared a conflict of interest relevant to the content of the
544 manuscript.

545

546 **Acknowledgements:** We would like to recognize the contribution of surgeons, nurses and
547 the medical team of the bariatric surgery program at IUCPQ. We would also like to
548 acknowledge the help of MRI technicians, Xavier Morel, Coordinator of the *Plateforme*
549 *d'imagerie avancée* at IUCPQ, Guillaume Gilbert, *Phillips*, Serge Simard, statistician, as well
550 as the help of Lucie Bouffard from Dr Carpentier lab for the measurement of gut hormones
551 and Mélanie Nadeau for the coordination of the study. Finally, we would sincerely like to
552 thank all the participants who took part in this study.

553

554

555

556 **References**

557

558 Al Massadi, O., López, M., Tschöp, M., Diéguez, C., & Nogueiras, R. (2017). Current
559 Understanding of the Hypothalamic Ghrelin Pathways Inducing Appetite and
560 Adiposity. *Trends Neurosci*, *40*(3), 167-180. doi:10.1016/j.tins.2016.12.003

561 Alfaro, F. J., Gavrieli, A., Saade-Lemus, P., Lioutas, V. A., Upadhyay, J., & Novak, V.
562 (2018). White matter microstructure and cognitive decline in metabolic syndrome: a
563 review of diffusion tensor imaging. *Metabolism*, *78*, 52-68.
564 doi:10.1016/j.metabol.2017.08.009

565 Alzaid, H., Simon, J. J., Brugnara, G., Vollmuth, P., Bendszus, M., & Friederich, H. C.
566 (2024). Hypothalamic subregion alterations in anorexia nervosa and obesity:
567 Association with appetite-regulating hormone levels. *Int J Eat Disord*, *57*(3), 581-
568 592. doi:10.1002/eat.24137

569 Arkink, E. B., Schmitz, N., Schoonman, G. G., van Vliet, J. A., Haan, J., van Buchem, M. A.,
570 . . . Kruit, M. C. (2017). The anterior hypothalamus in cluster headache. *Cephalalgia*,
571 *37*(11), 1039-1050. doi:10.1177/0333102416660550

572 Askarpour, M., Khani, D., Sheikhi, A., Ghaedi, E., & Alizadeh, S. (2019). Effect of Bariatric
573 Surgery on Serum Inflammatory Factors of Obese Patients: a Systematic Review and
574 Meta-Analysis. *Obes Surg*, *29*(8), 2631-2647. doi:10.1007/s11695-019-03926-0

575 Aukan, M. I., Coutinho, S., Pedersen, S. A., Simpson, M. R., & Martins, C. (2023).
576 Differences in gastrointestinal hormones and appetite ratings between individuals
577 with and without obesity-A systematic review and meta-analysis. *Obes Rev*, *24*(2),
578 e13531. doi:10.1111/obr.13531

579 Bedont, J. L., Newman, E. A., & Blackshaw, S. (2015). Patterning, specification, and
580 differentiation in the developing hypothalamus. *Wiley Interdiscip Rev Dev Biol*, *4*(5),
581 445-468. doi:10.1002/wdev.187

582 Bettcher, B. M., Walsh, C. M., Watson, C., Miller, J. W., Green, R., Patel, N., . . . Kramer, J.
583 H. (2013). Body mass and white matter integrity: the influence of vascular and
584 inflammatory markers. *PLoS One*, *8*(10), e77741. doi:10.1371/journal.pone.0077741

585 Biddinger, J. E., Lazarenko, R. M., Scott, M. M., & Simerly, R. (2020). Leptin suppresses
586 development of GLP-1 inputs to the paraventricular nucleus of the hypothalamus.
587 *Elife*, *9*. doi:10.7554/eLife.59857

588 Biertho, L., Biron, S., Hould, F. S., Lebel, S., Marceau, S., & Marceau, P. (2010). Is
589 biliopancreatic diversion with duodenal switch indicated for patients with body mass
590 index <50 kg/m²? *Surg Obes Relat Dis*, *6*(5), 508-514.
591 doi:10.1016/j.soard.2010.03.285

- 592 Biertho, L., Simon-Hould, F., Marceau, S., Lebel, S., Lescelleur, O., & Biron, S. (2016).
593 Current Outcomes of Laparoscopic Duodenal Switch. *Ann Surg Innov Res*, 10, 1.
594 doi:10.1186/s13022-016-0024-7
- 595 Billot, B., Bocchetta, M., Todd, E., Dalca, A. V., Rohrer, J. D., & Iglesias, J. E. (2020).
596 Automated segmentation of the hypothalamus and associated subunits in brain MRI.
597 *Neuroimage*, 223, 117287. doi:10.1016/j.neuroimage.2020.117287
- 598 Bocchetta, M., Gordon, E., Manning, E., Barnes, J., Cash, D. M., Espak, M., . . . Rohrer, J. D.
599 (2015). Detailed volumetric analysis of the hypothalamus in behavioral variant
600 frontotemporal dementia. *J Neurol*, 262(12), 2635-2642. doi:10.1007/s00415-015-
601 7885-2
- 602 Brown, S. S. G., Westwater, M. L., Seidlitz, J., Ziauddeen, H., & Fletcher, P. C. (2023).
603 Hypothalamic volume is associated with body mass index. *Neuroimage Clin*, 39,
604 103478. doi:10.1016/j.nicl.2023.103478
- 605 Caron, A., & Richard, D. (2017). Neuronal systems and circuits involved in the control of
606 food intake and adaptive thermogenesis. *Ann N Y Acad Sci*, 1391(1), 35-53.
607 doi:10.1111/nyas.13263
- 608 Castro, D. C., Cole, S. L., & Berridge, K. C. (2015). Lateral hypothalamus, nucleus
609 accumbens, and ventral pallidum roles in eating and hunger: interactions between
610 homeostatic and reward circuitry. *Front Syst Neurosci*, 9, 90.
611 doi:10.3389/fnsys.2015.00090
- 612 Coupe, P., Yger, P., Prima, S., Hellier, P., Kervrann, C., & Barillot, C. (2008). An optimized
613 blockwise nonlocal means denoising filter for 3-D magnetic resonance images. *IEEE*
614 *Trans Med Imaging*, 27(4), 425-441. doi:10.1109/tmi.2007.906087
- 615 Dagher, A. (2012). Functional brain imaging of appetite. *Trends Endocrinol Metab*, 23(5),
616 250-260. doi:10.1016/j.tem.2012.02.009
- 617 Farr, O. M., Sofopoulos, M., Tsoukas, M. A., Dincer, F., Thakkar, B., Sahin-Efe, A., . . .
618 Mantzoros, C. S. (2016). GLP-1 receptors exist in the parietal cortex, hypothalamus
619 and medulla of human brains and the GLP-1 analogue liraglutide alters brain activity
620 related to highly desirable food cues in individuals with diabetes: a crossover,
621 randomised, placebo-controlled trial. *Diabetologia*, 59(5), 954-965.
622 doi:10.1007/s00125-016-3874-y
- 623 Gastrointestinal surgery for severe obesity: National Institutes of Health Consensus
624 Development Conference Statement. (1992). *Am J Clin Nutr*, 55(2 Suppl), 615s-619s.
625 doi:10.1093/ajcn/55.2.615s
- 626 Ha, L. J., Yeo, H. G., Kim, Y. G., Baek, I., Baeg, E., Lee, Y. H., . . . Choi, H. J. (2024).
627 Hypothalamic neuronal activation in non-human primates drives naturalistic goal-
628 directed eating behavior. *Neuron*, 112(13), 2218-2230.e2216.
629 doi:10.1016/j.neuron.2024.03.029
- 630 Hankir, M. K., Rullmann, M., Seyfried, F., Preusser, S., Poppitz, S., Heba, S., . . . Pleger, B.
631 (2019). Roux-en-Y gastric bypass surgery progressively alters radiologic measures of

- 632 hypothalamic inflammation in obese patients. *JCI Insight*, 4(19).
633 doi:10.1172/jci.insight.131329
- 634 Huang, J., Chen, Y., Wang, X., Wang, C., Yang, J., & Guan, B. (2023). Change in
635 Adipokines and Gastrointestinal Hormones After Bariatric Surgery: a Meta-analysis.
636 *Obes Surg*, 33(3), 789-806. doi:10.1007/s11695-022-06444-8
- 637 Jenkinson, M., Beckmann, C. F., Behrens, T. E., Woolrich, M. W., & Smith, S. M. (2012).
638 FSL. *Neuroimage*, 62(2), 782-790. doi:10.1016/j.neuroimage.2011.09.015
- 639 Jensen, C. B., Pyke, C., Rasch, M. G., Dahl, A. B., Knudsen, L. B., & Secher, A. (2018).
640 Characterization of the Glucagonlike Peptide-1 Receptor in Male Mouse Brain Using
641 a Novel Antibody and In Situ Hybridization. *Endocrinology*, 159(2), 665-675.
642 doi:10.1210/en.2017-00812
- 643 Karra, E., Chandarana, K., & Batterham, R. L. (2009). The role of peptide YY in appetite
644 regulation and obesity. *J Physiol*, 587(1), 19-25. doi:10.1113/jphysiol.2008.164269
- 645 Kiss, D. S., Toth, I., Jocsak, G., Barany, Z., Bartha, T., Frenyo, L. V., . . . Zsarnovszky, A.
646 (2020). Functional Aspects of Hypothalamic Asymmetry. *Brain Sci*, 10(6).
647 doi:10.3390/brainsci10060389
- 648 Kreutzer, C., Peters, S., Schulte, D. M., Fangmann, D., Türk, K., Wolff, S., . . . Laudes, M.
649 (2017). Hypothalamic Inflammation in Human Obesity Is Mediated by Environmental
650 and Genetic Factors. *Diabetes*, 66(9), 2407-2415. doi:10.2337/db17-0067
- 651 Lei, Y., Liang, X., Sun, Y., Yao, T., Gong, H., Chen, Z., . . . Liu, T. (2024). Region-specific
652 transcriptomic responses to obesity and diabetes in macaque hypothalamus. *Cell*
653 *Metab*, 36(2), 438-453.e436. doi:10.1016/j.cmet.2024.01.003
- 654 Li, S., Liu, M., Cao, S., Liu, B., Li, D., Wang, Z., . . . Shi, Y. (2023). The Mechanism of the
655 Gut-Brain Axis in Regulating Food Intake. *Nutrients*, 15(17).
656 doi:10.3390/nu15173728
- 657 Maciejewski, M. L., Arterburn, D. E., Van Scoyoc, L., Smith, V. A., Yancy, W. S., Jr.,
658 Weidenbacher, H. J., . . . Olsen, M. K. (2016). Bariatric Surgery and Long-term
659 Durability of Weight Loss. *JAMA Surg*, 151(11), 1046-1055.
660 doi:10.1001/jamasurg.2016.2317
- 661 Matthews, D. R., Hosker, J. P., Rudenski, A. S., Naylor, B. A., Treacher, D. F., & Turner, R.
662 C. (1985). Homeostasis model assessment: insulin resistance and beta-cell function
663 from fasting plasma glucose and insulin concentrations in man. *Diabetologia*, 28(7),
664 412-419. doi:10.1007/bf00280883
- 665 Michaud, A., Dadar, M., Pelletier, M., Zeighami, Y., Garcia-Garcia, I., Iceta, S., . . . Dagher,
666 A. (2020). Neuroanatomical changes in white and grey matter after sleeve
667 gastrectomy. *Neuroimage*, 213, 116696. doi:10.1016/j.neuroimage.2020.116696
- 668 Morimoto, R., Satoh, F., Murakami, O., Totsune, K., Saruta, M., Suzuki, T., . . . Takahashi,
669 K. (2008). Expression of peptide YY in human brain and pituitary tissues. *Nutrition*,
670 24(9), 878-884. doi:10.1016/j.nut.2008.06.011

- 671 O'Brien, P. E., Hindle, A., Brennan, L., Skinner, S., Burton, P., Smith, A., . . . Brown, W.
672 (2019). Long-Term Outcomes After Bariatric Surgery: a Systematic Review and
673 Meta-analysis of Weight Loss at 10 or More Years for All Bariatric Procedures and a
674 Single-Centre Review of 20-Year Outcomes After Adjustable Gastric Banding. *Obes*
675 *Surg*, 29(1), 3-14. doi:10.1007/s11695-018-3525-0
- 676 Pané, A., Videla, L., Calvet, À., Viaplana, J., Vaqué-Alcázar, L., Ibarzabal, A., . . . Jiménez,
677 A. (2024). Hypothalamic Inflammation Improves Through Bariatric Surgery, and
678 Hypothalamic Volume Predicts Short-Term Weight Loss Response in Adults With or
679 Without Type 2 Diabetes. *Diabetes Care*, 47(7), 1162-1170. doi:10.2337/dc23-2213
- 680 Reichelt, A. C., Hare, D. J., Bussey, T. J., & Saksida, L. M. (2019). Perineuronal Nets:
681 Plasticity, Protection, and Therapeutic Potential. *Trends Neurosci*, 42(7), 458-470.
682 doi:10.1016/j.tins.2019.04.003
- 683 Rodrigues, L., Rezende, T. J. R., Wertheimer, G., Santos, Y., França, M., & Rittner, L.
684 (2022). A benchmark for hypothalamus segmentation on T1-weighted MR images.
685 *Neuroimage*, 264, 119741. doi:10.1016/j.neuroimage.2022.119741
- 686 Roger, C., Lasbleiz, A., Guye, M., Dutour, A., Gaborit, B., & Ranjeva, J. P. (2021). The Role
687 of the Human Hypothalamus in Food Intake Networks: An MRI Perspective. *Front*
688 *Nutr*, 8, 760914. doi:10.3389/fnut.2021.760914
- 689 Rosenberg, G. A., & Yang, Y. (2007). Vasogenic edema due to tight junction disruption by
690 matrix metalloproteinases in cerebral ischemia. *Neurosurg Focus*, 22(5), E4.
691 doi:10.3171/foc.2007.22.5.5
- 692 Rullmann, M., Preusser, S., Poppitz, S., Heba, S., Gousias, K., Hoyer, J., . . . Pleger, B.
693 (2019). Adiposity Related Brain Plasticity Induced by Bariatric Surgery. *Front Hum*
694 *Neurosci*, 13, 290. doi:10.3389/fnhum.2019.00290
- 695 Rullmann, M., Preusser, S., Poppitz, S., Heba, S., Hoyer, J., Schütz, T., . . . Pleger, B. (2018).
696 Gastric-bypass surgery induced widespread neural plasticity of the obese human
697 brain. *Neuroimage*, 172, 853-863. doi:10.1016/j.neuroimage.2017.10.062
- 698 Ruzok, T., Schmitz-Koep, B., Menegaux, A., Eves, R., Daamen, M., Boecker, H., . . .
699 Hedderich, D. M. (2022). Lower hypothalamus subunit volumes link with impaired
700 long-term body weight gain after preterm birth. *Front Endocrinol (Lausanne)*, 13,
701 1057566. doi:10.3389/fendo.2022.1057566
- 702 Salminen, P., Grönroos, S., Helmiö, M., Hurme, S., Juuti, A., Juusela, R., . . . Ovaska, J.
703 (2022). Effect of Laparoscopic Sleeve Gastrectomy vs Roux-en-Y Gastric Bypass on
704 Weight Loss, Comorbidities, and Reflux at 10 Years in Adult Patients With Obesity:
705 The SLEEVEPASS Randomized Clinical Trial. *JAMA Surg*, 157(8), 656-666.
706 doi:10.1001/jamasurg.2022.2229
- 707 Saper, C. B. (2012). Chapter 16 - Hypothalamus. In J. K. Mai & G. Paxinos (Eds.), *The*
708 *Human Nervous System (Third Edition)* (pp. 548-583). San Diego: Academic Press.
- 709 Saper, C. B., & Lowell, B. B. (2014). The hypothalamus. *Curr Biol*, 24(23), R1111-1116.
710 doi:10.1016/j.cub.2014.10.023

- 711 Schindler, S., Schönknecht, P., Schmidt, L., Anwander, A., Strauß, M., Trampel, R., . . .
712 Geyer, S. (2013). Development and evaluation of an algorithm for the computer-
713 assisted segmentation of the human hypothalamus on 7-Tesla magnetic resonance
714 images. *PLoS One*, 8(7), e66394. doi:10.1371/journal.pone.0066394
- 715 Schur, E. A., Melhorn, S. J., Oh, S. K., Lacy, J. M., Berkseth, K. E., Guyenet, S. J., . . .
716 Maravilla, K. R. (2015). Radiologic evidence that hypothalamic gliosis is associated
717 with obesity and insulin resistance in humans. *Obesity (Silver Spring)*, 23(11), 2142-
718 2148. doi:10.1002/oby.21248
- 719 Sewaybricker, L. E., Huang, A., Chandrasekaran, S., Melhorn, S. J., & Schur, E. A. (2023).
720 The Significance of Hypothalamic Inflammation and Gliosis for the Pathogenesis of
721 Obesity in Humans. *Endocr Rev*, 44(2), 281-296. doi:10.1210/edrev/bnac023
- 722 Sled, J. G., Zijdenbos, A. P., & Evans, A. C. (1998). A nonparametric method for automatic
723 correction of intensity nonuniformity in MRI data. *IEEE Trans Med Imaging*, 17(1),
724 87-97. doi:10.1109/42.668698
- 725 Thaler, J. P., Guyenet, S. J., Dorfman, M. D., Wisse, B. E., & Schwartz, M. W. (2013).
726 Hypothalamic inflammation: marker or mechanism of obesity pathogenesis?
727 *Diabetes*, 62(8), 2629-2634. doi:10.2337/db12-1605
- 728 Thomas, K., Beyer, F., Lewe, G., Zhang, R., Schindler, S., Schönknecht, P., . . . Witte, A. V.
729 (2019). Higher body mass index is linked to altered hypothalamic microstructure. *Sci*
730 *Rep*, 9(1), 17373. doi:10.1038/s41598-019-53578-4
- 731 Toshinai, K., Date, Y., Murakami, N., Shimada, M., Mondal, M. S., Shimbara, T., . . .
732 Nakazato, M. (2003). Ghrelin-induced food intake is mediated via the orexin
733 pathway. *Endocrinology*, 144(4), 1506-1512. doi:10.1210/en.2002-220788
- 734 Tuulari, J. J., Karlsson, H. K., Antikainen, O., Hirvonen, J., Pham, T., Salminen, P., . . .
735 Nummenmaa, L. (2016). Bariatric Surgery Induces White and Grey Matter Density
736 Recovery in the Morbidly Obese: A Voxel-Based Morphometric Study. *Hum Brain*
737 *Mapp*, 37(11), 3745-3756. doi:10.1002/hbm.23272
- 738 van de Sande-Lee, S., Melhorn, S. J., Rachid, B., Rodvalho, S., De-Lima-Junior, J. C.,
739 Campos, B. M., . . . Velloso, L. A. (2020). Radiologic evidence that hypothalamic
740 gliosis is improved after bariatric surgery in obese women with type 2 diabetes. *Int J*
741 *Obes (Lond)*, 44(1), 178-185. doi:10.1038/s41366-019-0399-8
- 742 Wang, Y., Ji, G., Hu, Y., Li, G., Ding, Y., Hu, C., . . . Zhang, Y. (2020). Laparoscopic sleeve
743 gastrectomy induces sustained changes in gray and white matter brain volumes and
744 resting functional connectivity in obese patients. *Surg Obes Relat Dis*, 16(1), 1-9.
745 doi:10.1016/j.soard.2019.09.074
- 746 Willeumier, K. C., Taylor, D. V., & Amen, D. G. (2011). Elevated BMI is associated with
747 decreased blood flow in the prefrontal cortex using SPECT imaging in healthy adults.
748 *Obesity (Silver Spring)*, 19(5), 1095-1097. doi:10.1038/oby.2011.16

- 749 Xie, Y., & Dorsky, R. I. (2017). Development of the hypothalamus: conservation,
750 modification and innovation. *Development*, *144*(9), 1588-1599.
751 doi:10.1242/dev.139055
- 752 Zeighami, Y., Iceta, S., Dadar, M., Pelletier, M., Nadeau, M., Biertho, L., . . . Michaud, A.
753 (2021). Spontaneous neural activity changes after bariatric surgery: A resting-state
754 fMRI study. *Neuroimage*, *241*, 118419. doi:10.1016/j.neuroimage.2021.118419
755